Supplementary Information: Revealing Formic Acid Adsorption Geometries on Magnetite (001) and (111) Surfaces by IRRAS Line Shape Analysis

Heshmat Noei[1*], Marcus Creutzburg[1], Gregor Vonbun-Feldbauer[2,3,4], and Andreas Stierle[1,5]

[1]*Deutsches Elektronen-Synchrotron DESY, Center of X-ray and Nano Science (CXNS), Notkestr. 85, 22607 Hamburg, Germany*
[2]*Hamburg University of Technology (TUHH), Institute for Interface Physics and Engineering, Am Irrgarten 3-9, 21073 Hamburg, Germany*
[3]*Hamburg University of Technology (TUHH), Institute of Advanced Ceramics, Denickestr. 15, 21073 Hamburg, Germany*
[4]*Helmholtz-Zentrum Hereon, Institute of Surface Science, Max-Planck-Str. 1, 21502 Geesthacht, Germany*
[5]*University of Hamburg, Department of Physics, Luruper Chaussee 149, 22607 Hamburg, Germany*

April 20, 2026

Contents

S1 Calculated Vibrational Spectra

The accuracy of the calculated vibrational wavenumbers for specific modes depends strongly on the chosen approximations. One approximation is the chosen level of theory for the electronic structure calculation or more general for the atomistic simulation method. Here, density functional theory (DFT) calculations were done with the generalized gradient approximation (GGA) for the exchange-correlation (XC) functional. Specifically, PBE [1] was used as XC functional. PBE often underestimates bonds strengths and force constants [2, 3] which causes underestimated (red-shifted) vibrational frequencies and wavenumbers. Increasing the level of theory within the framework of DFT can help here; however, there is no guarantee. E.g., metaGGAs like SCAN [4] failed to significantly improve over GGA results for CO adsorbed on ceria surfaces [5], while it was shown that the hybrid functional HSE06 [6] works very well for that specific application [7]. Going beyond the level of DFT can yield more accurate vibrational frequencies at significantly increased computational costs, e.g., Alecu et al. [8] showed that calculations based on coupled cluster theory reproduced experimental results for the F38/10 database including 15 small molecules more reliably than DFT. Current advances from the field of machine learning are very promising but those are not discussed here.

On the other hand, the chosen approximation for the vibrations is important. Here, the harmonic approximation was used which neglects anharmonicity and therefore usually overestimates vibrational frequencies and wavenumbers. This corresponds to a blue shift versus experimental results. Since the two approximations often show different signs, a partial compensation can take place. The resulting effect however depends on the vibrational mode and the involved bonds as exemplified in the following by literature results all obtained using DFT.

Porezag and Pederson presented calculated and experimental vibrational frequencies for a set of small molecules, namely 4 small hydrocarbons and water, for LDA and GGA functionals [9]. Based on that data, Skibinski *et al.* [10] calculated an average red shift of 2.8 % for GGA functionals. Investigating phenylphosphinates and benzoates adsorbed on rutile TiO_2 (110) Skibinski *et al.* observed that calculated (using PBE) O-C-O stretching modes of the benzoates were only red-shifted by about 1 % versus their experimental results, while the O-P-O stretching modes appeared red-shifted by about 3–5 %. Similarly, Li *et al.* [11] observed a red shift of the calculated (PBE) frequency of the stretching mode of a free CO molecule and of CO adsorbed on a Fe_3O_4 (111) surface of about 1 % and 1.5 %, respectively, versus experimental results. In Würger *et al.*, acetone adsorbed on TiO_2 (110) was studied experimentally and computationally using DFT with three different GGA-level XC functionals (PBE, PBEsol [12], PW91 [13]) and one van-der-Waals-corrected functional (optB88-vdW [14, 15]). For the C-C and C-O stretching modes, the calculated frequencies were red-shifted by about 1–1.8 % and 1.8–2.4 %, respectively, versus the experimental results depending on the XC functional. While results for the three standard GGA functionals deviated by less than 0.3 % from each other, the deviation from the vdW-functional was increased to about 0.5–1 %. There is however no clear superiority, since the GGA functional performed better for the C-C mode while the vdW-functional predicted values closer to the experimental results for the C-O mode. Modes including hydrogen showed larger deviations as expected because of the harmonic approximation. For formic acid dissociatively adsorbed on Fe_3O_4 (001) [16] and (111) [17], a red shift of the calculated (PBE) O-C-O stretching modes versus experimental results by about 1–3.5 % was observed for different binding modes. Symmetric stretching modes were found to be deviating more strongly from the experimental values

than asymmetric stretching modes. In summary, all those results from the literature suggest that calculated vibrational frequencies of modes containing C-O bonds are red shifted versus experimental results by about 1–3.5 % using DFT and GGA XC-functionals.

Additional approximations like neglecting nuclear quantum effects [18] are not be discussed here in more detail, even though they can be important for some vibrations particularly those including light elements as hydrogen as mentioned in the main manuscript.

Calculated vibrational spectra and the corresponding wavenumbers and rela-tive intensities are presented for molecularly and dissociatively adsorbed formic acid on magnetite (001) and (111) surfaces. Computational details can be found in the main manuscript. Only adsorption geometries that were not studied before in our previous publications are shown here. For details on the other geometries and vibrational spectra please refer to [16, 17] and the PhD thesis by Kai Sellschopp [19]. The atomic coordinates (VASP POSCAR format) used as input for the calculations and snapshots (xyz files) of the vibrational motions can be found in the online repository TORE [20].

The following adsorption geometries are shown here:

- Fe_3O_4 DBT-(001) - molecular adsorption - monodentate mode: Fig. S1, Fig. S2, Tab. S1
- Fe_3O_4 DBT-(001) - molecular adsorption - quasi-bidentate mode (via rest group H): Fig. S3, Fig. S4, Tab. S2
- Fe_3O_4 DBT-(001) - dissociative adsorption - monodentate mode: Fig. S5, Fig. S6, Tab. S3
- Fe_3O_4 tet1-(111) - molecular adsorption - monodentate mode: Fig. S7, Fig. S8, Tab. S4
- Fe_3O_4 tet1-(111) - molecular adsorption - quasi-bidentate mode (via rest group H): Fig. S11, Fig. S12, Tab. S6
- Fe_3O_4 tet1-(111) - dissociative adsorption - monodentate mode: Fig. S9, Fig. S10, Tab. S5
- Fe_3O_4 tet1-(111) - dissociative adsorption - quasi-bidentate mode (via rest group H): Fig. S13, Fig. S14, Tab. S7

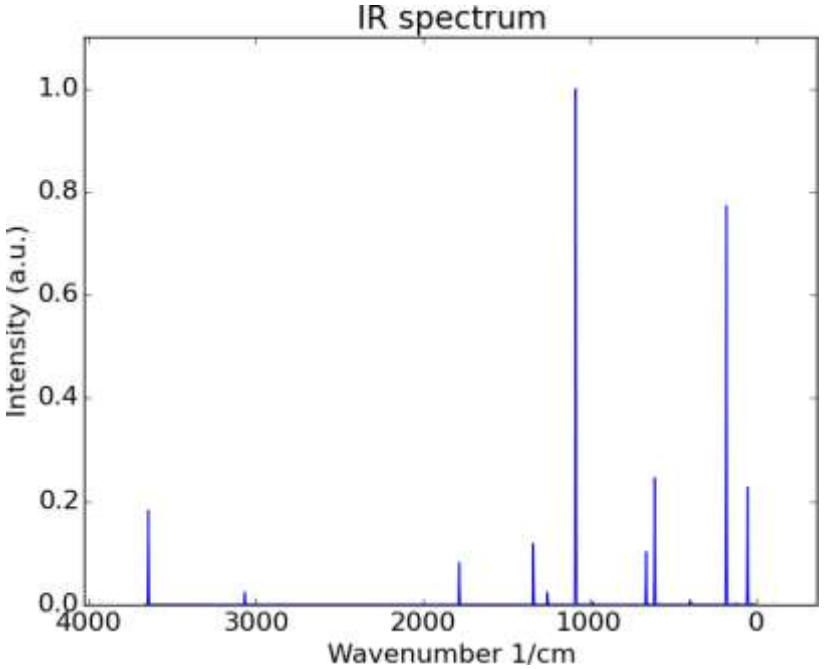

Figure S1 Complete calculated vibrational spectrum of molecularly adsorbed formic acid at Fe_3O_4 DBT-(001) surface with a monodentate binding mode. A zoom into the here most relevant wavenumber region is shown in Fig. S2. Wavenumbers and relative intensities are presented in Tab. S1.

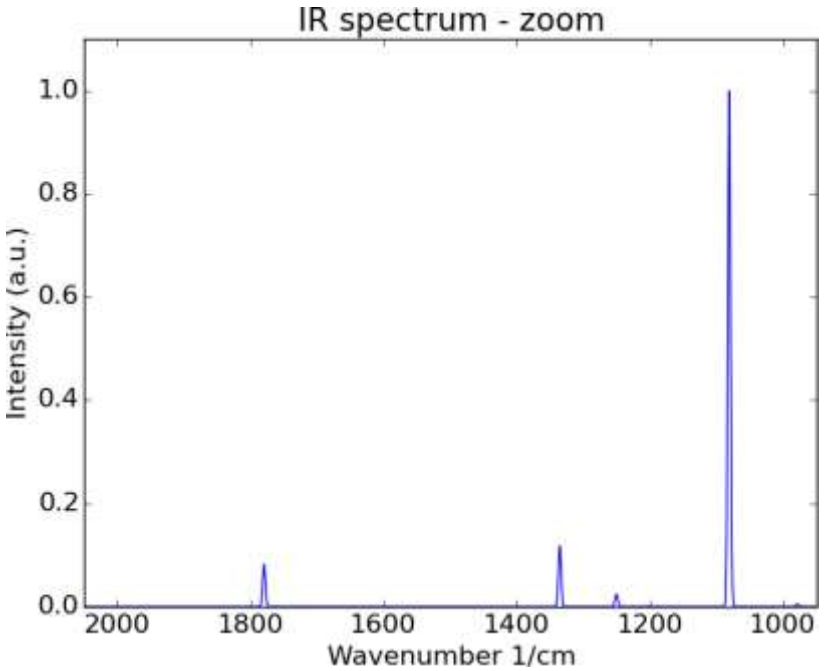

Figure S2 Zoom into calculated vibrational spectrum of molecularly adsorbed formic acid at Fe_3O_4 DBT-(001) surface with a monodentate binding mode.

Mode	Wavenumber (cm^{-1})	Relative Intensity
001	3644.4	0.183
002	3065.2	0.024
003	1779.5	0.082
004	1335.6	0.118
005	1250.5	0.024
006	1081.2	1.000
007	978.8	0.005
008	658.6	0.103
009	607.2	0.246
010	393.7	0.009
011	192.7	0.001
012	177.4	0.774
013	120.9	0.003
014	50.0	0.228
015	23.1	0.002

Table S1 Calculated vibrational modes of molecularly adsorbed formic acid at Fe_3O_4 DBT-(001) surface with a monodentate binding mode with their wavenumber in cm^{-1} and the relative intensity scaled to the highest peak in this spectrum. Plotted in Fig. S1.

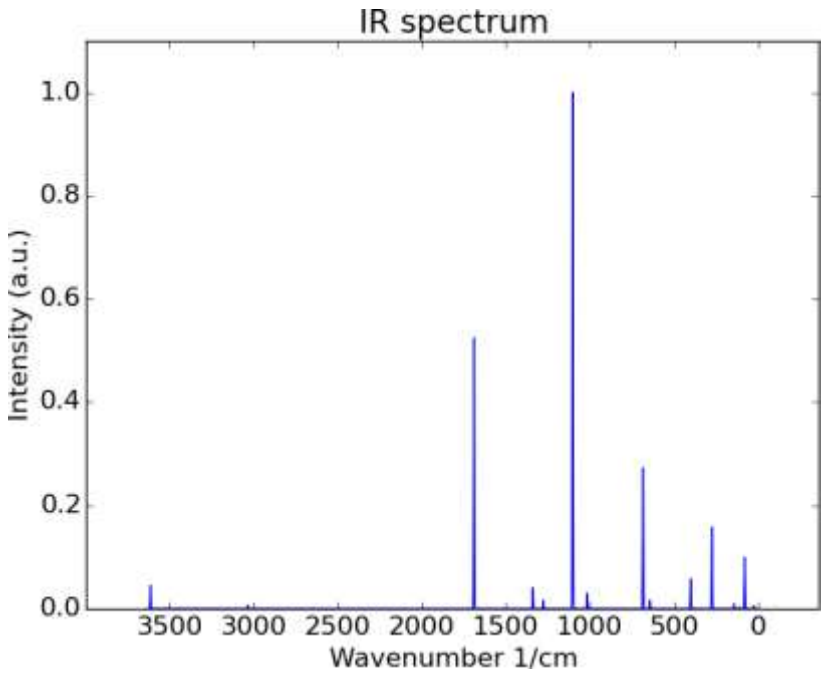

Figure S3 Complete calculated vibrational spectrum of molecularly adsorbed formic acid at Fe_3O_4 DBT-(001) surface with a quasi-bidentate binding mode via the rest group hydrogen. A zoom into the here most relevant wavenumber region is shown in Fig. S4. Wavenumbers and relative intensities are presented in Tab. S2.

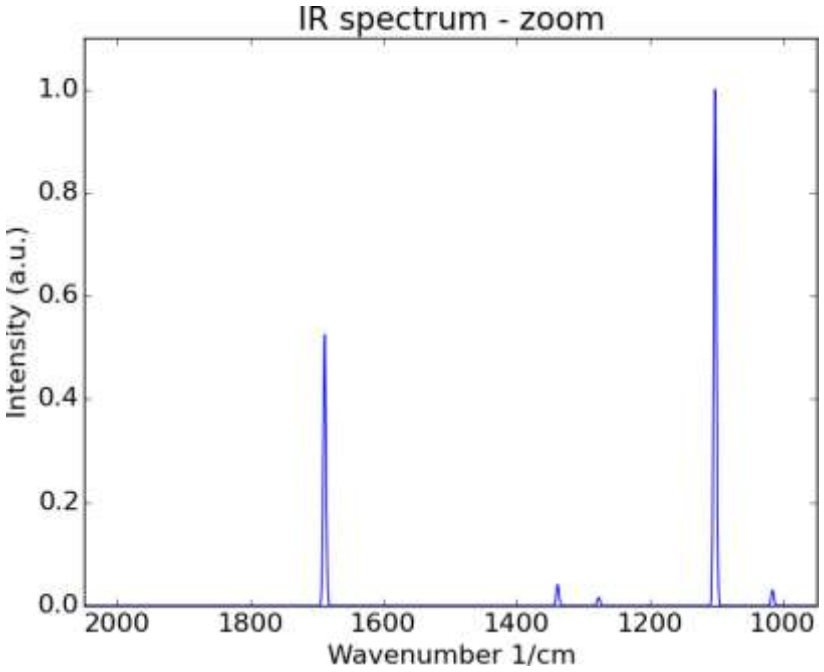

Figure S4 Zoom into calculated vibrational spectrum of molecularly adsorbed formic acid at Fe_3O_4 DBT-(001) surface with a quasi-bidentate binding mode via the rest group hydrogen.

Mode	Wavenumber (cm^{-1})	Relative Intensity
001	3611.4	0.045
002	3032.2	0.006
003	1688.6	0.525
004	1338.7	0.041
005	1277.0	0.016
006	1102.4	1.000
007	1016.2	0.030
008	684.4	0.273
009	643.2	0.016
010	401.0	0.058
011	275.1	0.158
012	142.8	0.009
013	107.7	0.003
014	79.8	0.099
015	25.0	0.005

Table S2 Calculated vibrational modes of molecularly adsorbed formic acid at Fe_3O_4 DBT-(001) surface with a quasi-bidentate binding mode via the rest group hydrogen with their wavenumber in cm^{-1} and the relative intensity scaled to the highest peak in this spectrum. Plotted in Fig. S3.

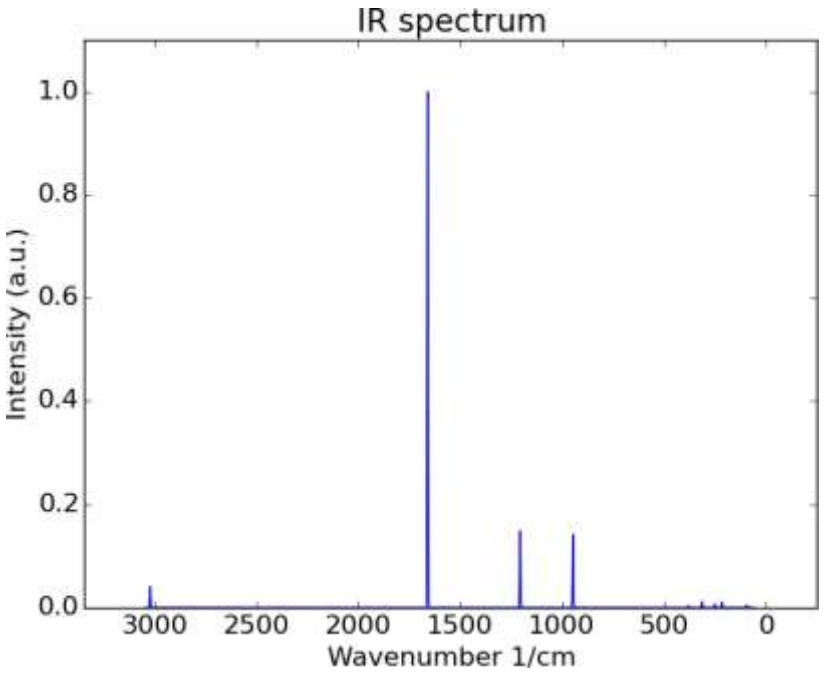

Figure S5 Complete calculated vibrational spectrum of adsorbed formate at Fe_3O_4 DBT-(001) surface with a monodentate binding mode. A zoom into the here most relevant wavenumber region is shown in Fig. S6. Wavenumbers and relative intensities are presented in Tab. S3.

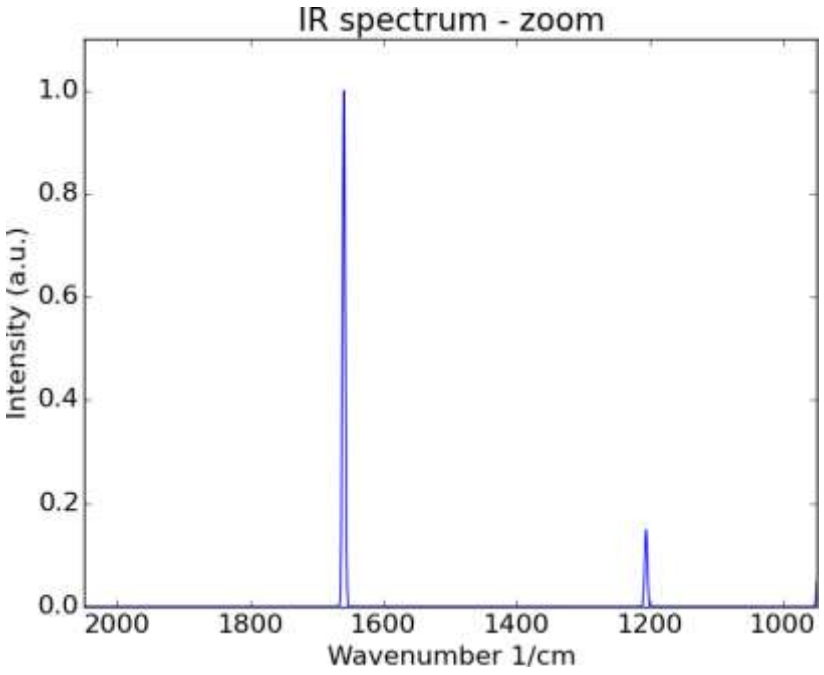

Figure S6 Zoom into calculated vibrational spectrum of adsorbed formate at Fe_3O_4 DBT-(001) surface with a monodentate binding mode.

Mode	Wavenumber (cm^{-1})	Relative Intensity
001	3020.1	0.041
002	1659.8	1.000
003	1206.1	0.149
004	946.9	0.142
005	916.0	0.000
006	380.4	0.004
007	313.2	0.012
008	251.1	0.007
009	216.1	0.011
010	198.5	0.000
011	95.4	0.005
012	77.0	0.001

Table S3 Calculated vibrational modes of adsorbed formate at Fe_3O_4 DBT-(001) surface with a monodentate binding mode with their wavenumber in cm^{-1} and the relative intensity scaled to the highest peak in this spectrum. Plotted in Fig. S5.

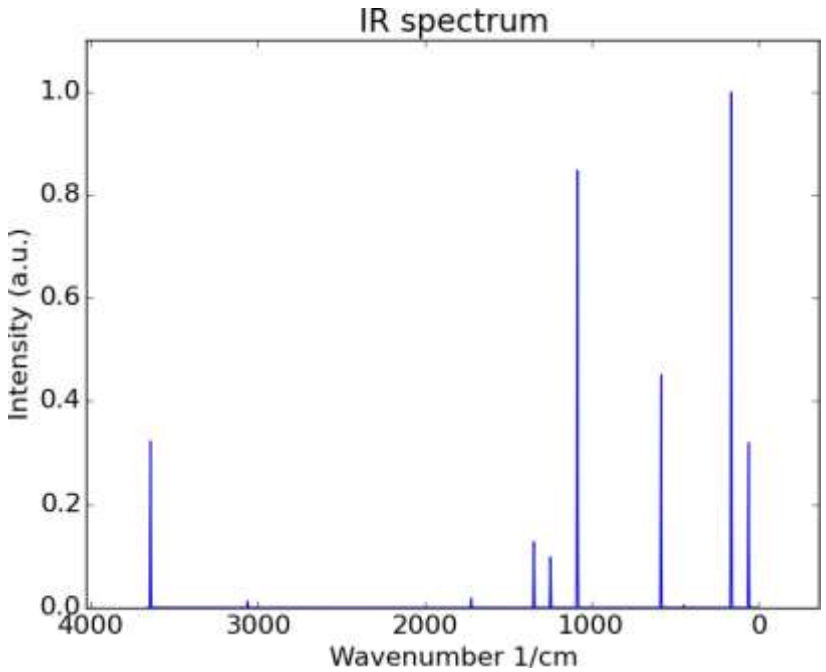

Figure S7 Complete calculated vibrational spectrum of molecularly adsorbed formic acid at Fe_3O_4 tet1-(111) surface with a monodentate binding mode. A zoom into the here most relevant wavenumber region is shown in Fig. S8. Wavenumbers and relative intensities are presented in Tab. S4.

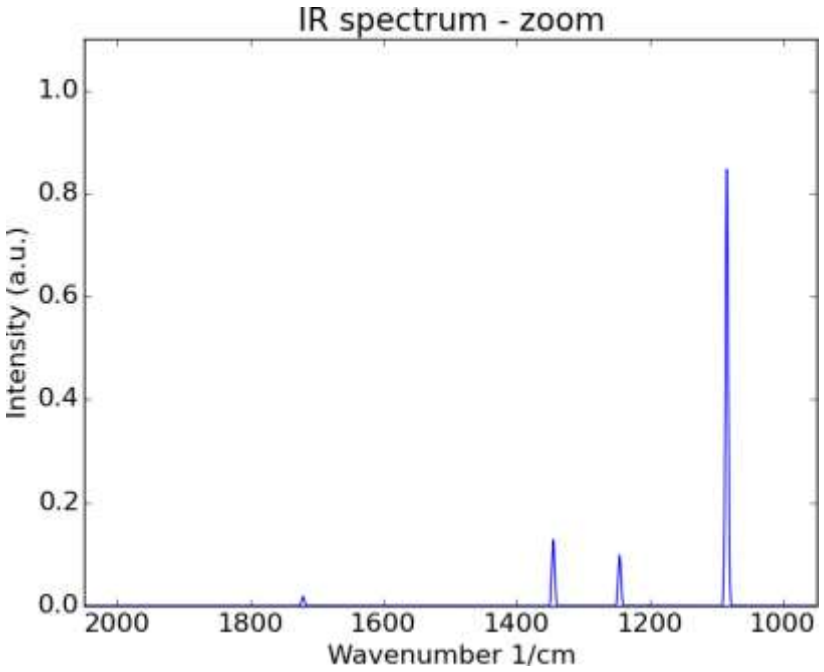

Figure S8 Zoom into calculated vibrational spectrum of molecularly adsorbed formic acid at Fe_3O_4 tet1-(111) surface with a monodentate binding mode.

Mode	Wavenumber (cm^{-1})	Relative Intensity
001	3641.5	0.323
002	3060.2	0.013
003	1721.0	0.018
004	1345.3	0.128
005	1245.7	0.098
006	1084.8	0.848
007	889.6	0.000
008	620.2	0.000
009	583.6	0.452
010	449.7	0.005
011	200.0	0.000
012	163.6	1.000
013	95.7	0.000
014	59.7	0.320
015	26.9	0.000

Table S4 Calculated vibrational modes of molecularly adsorbed formic acid at Fe_3O_4 tet1-(111) surface with a monodentate binding mode with their wavenumber in cm^{-1} and the relative intensity scaled to the highest peak in this spectrum. Plotted in Fig. S7.

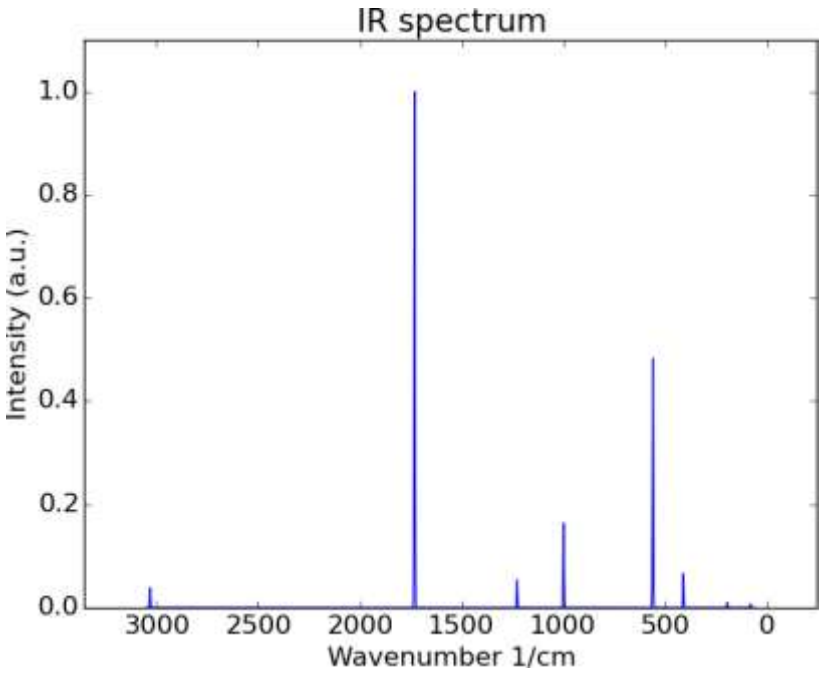

Figure S9 Complete calculated vibrational spectrum of adsorbed formate at Fe_3O_4 tet1-(111) surface with a monodentate binding mode. A zoom into the here most relevant wavenumber region is shown in Fig. S10. Wavenumbers and relative intensities are presented in Tab. S5.

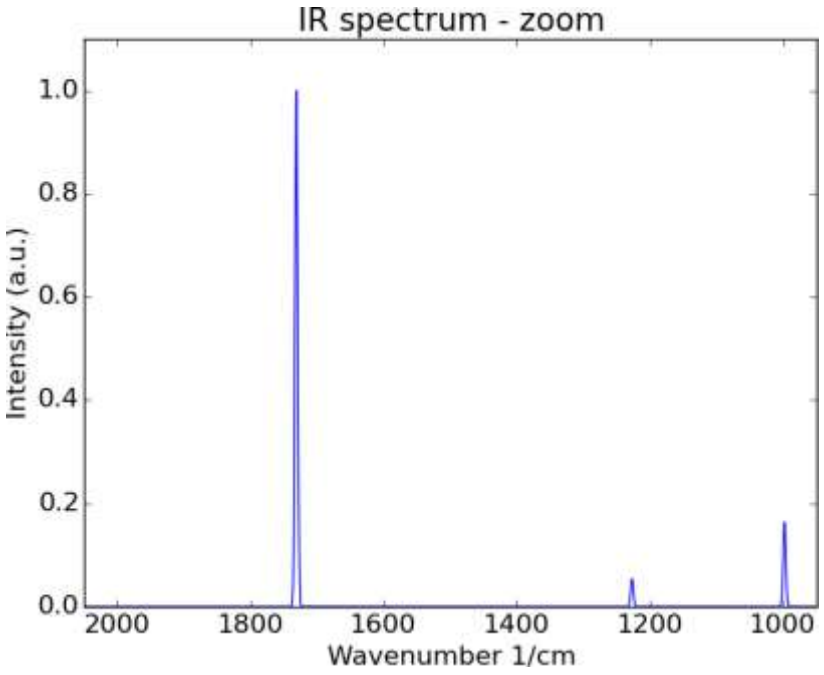

Figure S10 Zoom into calculated vibrational spectrum of adsorbed formate at Fe_3O_4 tet1-(111) surface with a monodentate binding mode.

Mode	Wavenumber (cm^{-1})	Relative Intensity
001	3031.7	0.038
002	1731.1	1.000
003	1227.1	0.054
004	998.2	0.164
005	919.6	0.000
006	558.9	0.483
007	409.5	0.066
008	276.5	0.000
009	215.6	0.000
010	193.2	0.010
011	82.2	0.000
012	80.1	0.007

Table S5 Calculated vibrational modes of adsorbed formate at Fe_3O_4 tet1-(111) surface with a monodentate binding mode with their wavenumber in cm^{-1} and the relative intensity scaled to the highest peak in this spectrum. Plotted in Fig. S9.

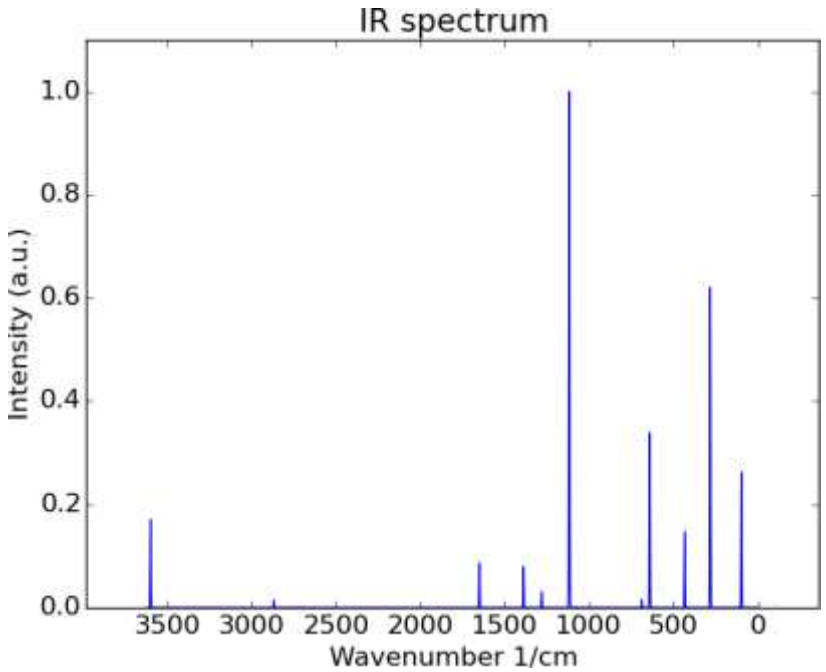

Figure S11 Complete calculated vibrational spectrum of molecularly adsorbed formic acid at Fe_3O_4 tet1-(111) surface with a quasi-bidentate binding mode via the rest group hydrogen. A zoom into the here most relevant wavenumber region is shown in Fig. S12. Wavenumbers and relative intensities are presented in Tab. S6.

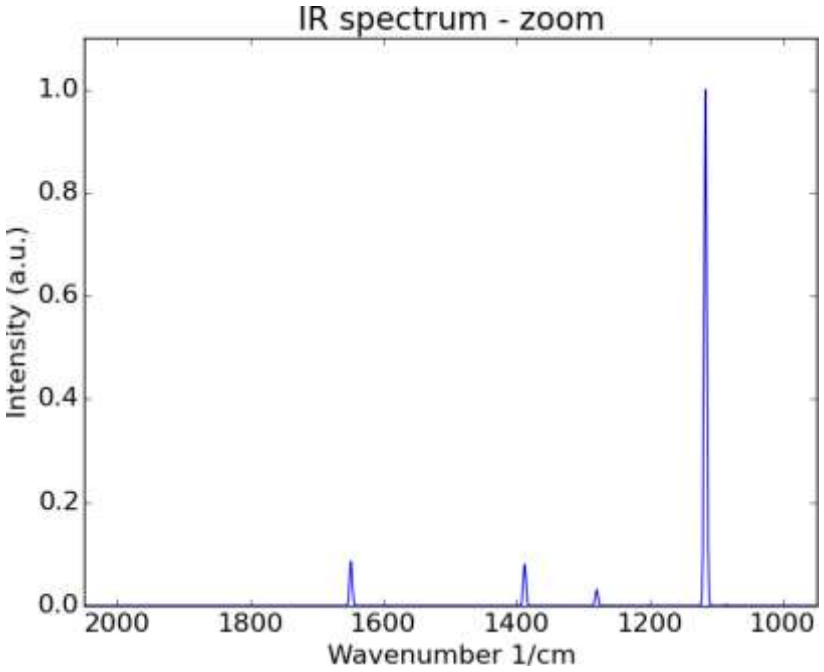

Figure S12 Zoom into calculated vibrational spectrum of molecularly adsorbed formic acid at Fe_3O_4 tet1-(111) surface with a quasi-bidentate binding mode via the rest group hydrogen.

Mode	Wavenumber (cm^{-1})	Relative Intensity
001	3597.3	0.171
002	2866.8	0.014
003	1649.1	0.086
004	1388.3	0.080
005	1280.1	0.031
006	1116.8	1.000
007	1086.0	0.002
008	687.5	0.016
009	640.4	0.339
010	433.3	0.147
011	282.0	0.621
012	157.5	0.000
013	109.9	0.002
014	97.0	0.262
015	22.4	0.001

Table S6 Calculated vibrational modes of molecularly adsorbed formic acid at Fe_3O_4 tet1-(111) surface with a quasi-bidentate binding mode via the rest group hydrogen with their wavenumber in cm^{-1} and the relative intensity scaled to the highest peak in this spectrum. Plotted in Fig. S11.

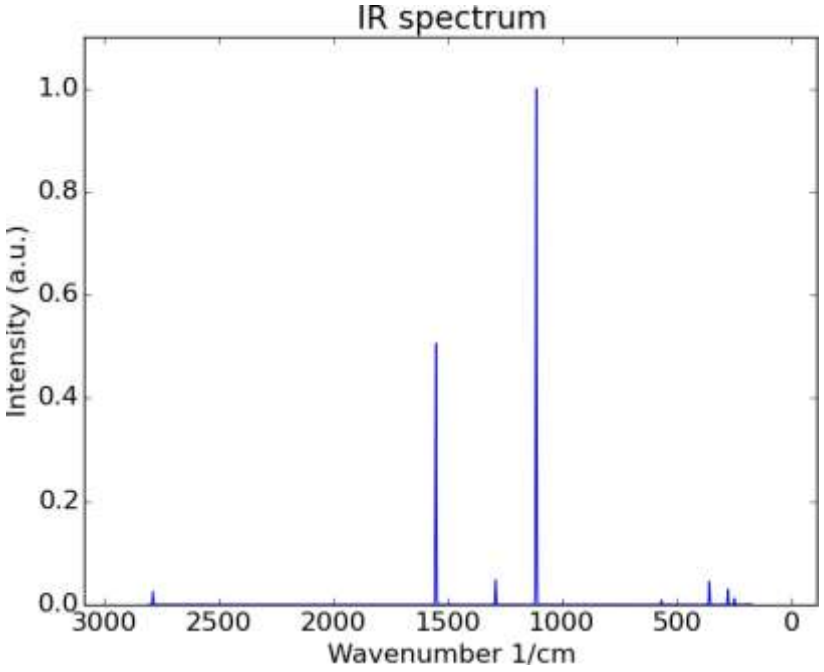

Figure S13 Complete calculated vibrational spectrum of adsorbed formate at Fe_3O_4 tet1-(111) surface with a quasi-bidentate binding mode via the rest group hydrogen. A zoom into the here most relevant wavenumber region is shown in Fig. S14. Wavenumbers and relative intensities are presented in Tab. S7.

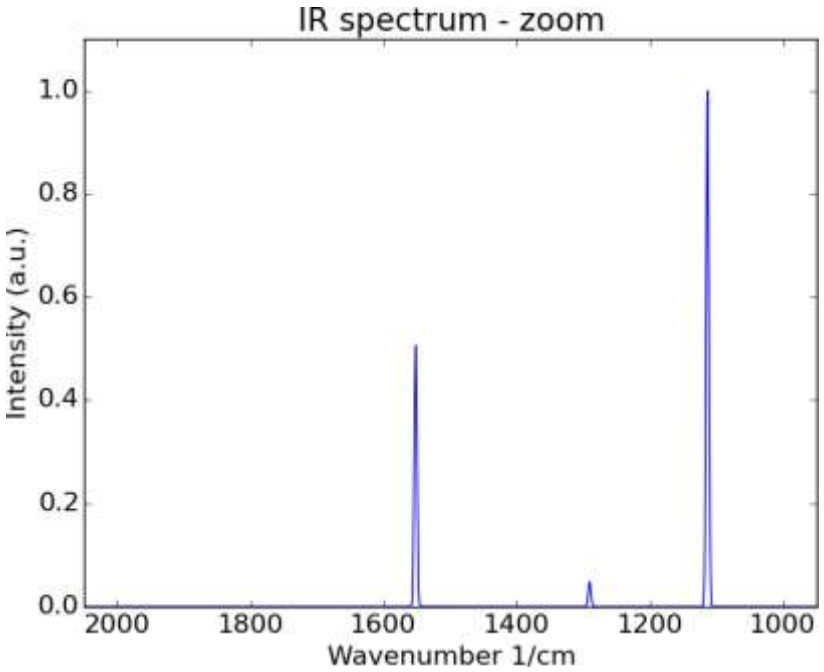

Figure S14 Zoom into calculated vibrational spectrum of adsorbed formate at Fe_3O_4 tet1-(111) surface with a quasi-bidentate binding mode via the rest group hydrogen.

Mode	Wavenumber (cm^{-1})	Relative Intensity
001	2786.8	0.025
002	1552.0	0.506
003	1290.9	0.048
004	1113.8	1.000
005	1014.2	0.000
006	652.2	0.000
007	567.4	0.009
008	357.9	0.045
009	303.0	0.000
010	276.8	0.030
011	248.4	0.012
012	191.0	0.002

Table S7 Calculated vibrational modes of adsorbed formate at Fe_3O_4 tet1-(111) surface with a quasi-bidentate binding mode via the rest group hydrogen with their wavenumber in cm^{-1} and the relative intensity scaled to the highest peak in this spectrum. Plotted in Fig. S13.

S2 Fano fitting

Table S8 Fit parameter overview for selected Fano lines.

Fit parameter	magnetite (111) ν_s(OCO) chel.	magnetite (111) ν_s(OCO) qbt.	magnetite (001) ν_s(OCO) bb.	magnetite (001) δ(CH)
θ (°)	74.4	75.2	75.5	75.5
ν_0 (cm^{-1})	1380.57	1336.87	1372.00	1372.67
γ (cm^{-1})	4.73	6.03	9.12	4.28
N_s	0.008	0.008	0.026	0.020
α_v	0.65	1.46	1.22	0.42

Fit parameter	magnetite (001) ν_{as}^{tet}(OCO)	magnetite (001) ν_{as}^{int}(OCO)
θ (°)	77.0	77.0
ν_0 (cm^{-1})	1552.10	1541.47
γ (cm^{-1})	8.91	9.97
N_s	0.002	0.007
α_v	1.3	1.05

References

[1] J. P. Perdew, K. Burke, and M. Ernzerhof, *Phys. Rev. Lett.*, 1996, **77**(18), 3865–3868.

[2] B. Grabowski, T. Hickel, and J. Neugebauer, *Phys. Rev. B*, 2007, **76**(2), 024309.

[3] C. Stampfl and C. G. Van de Walle, *Phys. Rev. B*, 1999, **59**(8), 5521–5535.

[4] J. Sun, A. Ruzsinszky, and J. P. Perdew, *Phys. Rev. Lett.*, 2015, **115**, 036402.

[5] A. Contreras-Payares, P. G. Lustemberg, and M. V. Ganduglia-Pirovano, *J. Chem. Phys.*, 2025, **163**(2), 024701.

[6] A. V. Krukau, O. A. Vydrov, A. F. Izmaylov, and G. E. Scuseria, *J. Chem. Phys.*, 2006, **125**(22), 224106.

[7] P. G. Lustemberg, C. Yang, Y. Wang, C. Wöll, and M. V. Ganduglia-Pirovano, *J. Chem. Phys.*, 2023, **159**(3), 034704.

[8] I. M. Alecu, J. Zheng, Y. Zhao, and D. G. Truhlar, *J. Chem. Theory Comput.*, 2010, **6**(9), 2872–2887.

[9] D. Porezag and M. R. Pederson, *Phys. Rev. B*, 1996, **54**(11), 7830–7836.

[10] E. S. Skibinski, W. J. I. DeBenedetti, and M. A. Hines, *J. Phys. Chem. C*, 2017, **121**(26), 14213–14221.

[11] X. Li, J. Paier, J. Sauer, F. Mirabella, E. Zaki, F. Ivars-Barceló, S. Shaikhutdinov, and H.-J. Freund, June , 2017, **122**(2), 527–533.

[12] J. P. Perdew, A. Ruzsinszky, G. I. Csonka, O. A. Vydrov, G. E. Scuseria, L. A. Constantin, X. Zhou, and K. Burke, *Phys. Rev. Lett.*, 2008, **100**, 136406.

[13] J. P. Perdew and Y. Wang, *Physical Review B*, 1992, **45**(23), 13244.

[14] J. Klimeš, D. R. Bowler, and A. Michaelides, *Journal of Physics: Condensed Matter*, 2010, **22**(2), 022201.

[15] J. Klimeš, D. R. Bowler, and A. Michaelides, *Phys. Rev. B*, 2011, **83**(19), 195131.

[16] B. Arndt, K. Sellschopp, M. Creutzburg, E. Grånäs, K. Krausert, V. Vonk, S. Müller, H. Noei, G. Vonbun-Feldbauer, and A. Stierle, *Comm. Chem.*, 2019, **2**(92).

[17] M. Creutzburg, K. Sellschopp, S. Tober, E. Grånäs, V. Vonk, W. Mayr-Schmölzer, S. Müller, H. Noei, G. B. Vonbun-Feldbauer, and A. Stierle, *J. Phys. Chem. Lett.*, 2021, **12**(15), 3847–3852.

[18] M. Rossi, *J. Chem. Phys.*, 2021, **154**(17), 170902.

[19] K. Sellschopp *Understanding interfaces in metal-oxide/organic-acid hybrid materials from first-principles calculations.* PhD thesis, TU Hamburg, Germany, 2021.

[20] G. Vonbun-Feldbauer and K. Sellschopp, Data for "Computational vibrational spectra for formic acid adsorbed on magnetite surfaces from DFT calculations". TUHH Open Research (TORE) Repository, DOI: 10.15480/882.15191, 2025.